WAVE MODE IDENTIFICATION BY THE CLUSTER SATELLITES IN THE FORESHOCK REGION

Anders Tjulin[1], Elizabeth Lucek[1], and Mats André[2]

[1] *Imperial College, Space & Atmospheric Physics, Blackett Laboratory, Prince Consort Rd, London SW7 2BZ, UK, a.tjulin@imperial.ac.uk, e.lucek@imperial.ac.uk*
[2] *Swedish Institute of Space Physics, Box 537, 751 21 Uppsala, Sweden, mats.andre@irfu.se*

ABSTRACT

The plasma waves and fluctuations in the Earth's fore-shock region have been explored using Cluster data. In this case study we have combinesd multi-point measurements of the magnetic field, from the FluxGate Magnetometer (FGM) instrument, and the electric field, from the Electric Field and Wave (EFW) instrument, and used them in order to identify the encountered wave mode. The k-filtering technique has been employed for the detailed examination of the wave power density distribution in frequency and wave-vector space. This method also provided the possibility to transform the wave field data into the plasma frame of reference, which enables comparison with plasma theory and the eventual identification of the plasma wave mode. The combination of FGM and EFW data has allowed for investigation of the ratio between the electric and magnetic power of the waves and it also enhanced the k-filtering method compared with the case when only data from one instrument is used.

Key words: Solar wind; foreshock; bow-shock and magnetosheath.

1. INTRODUCTION

The Earth's foreshock contains large amplitude ultra low frequency (ULF) waves. They are frequently observed by spacecraft and they have a typical period of about 30 s. These waves are generated by instabilities between the solar wind plasma and ions streaming back from the bow shock, and the amplitude of the magnetic fluctuations are of the same order of magnitude as the background magnetic field. This is a case study of the ULF waves for one event and we have applied both single spacecraft methods and multi-spacecraft methods, such as the k-filtering technique [1], for the identification of the wave mode of the ULF emissions. We have used wave data from the FluxGate Magnetometer (FGM) and the Electric Field

and Wave (EFW) instruments [2, 3] on Cluster for the analysis. This study included the first k-filtering study using the combined FGM and EFW datasets.

2. THE ULF WAVE EVENT

The data we have used are from 13 May 2005 with the Cluster satellites located in the foreshock region with inter-spacecraft separation of ahout 1000 km. The spacecraft constellation was favourable for multi-spacecraft studies with elongation 0.25 and planarity 0.31 [4] which means that the spacecraft were located at the apexes of a nearlty regular tetrahedron. This constellation made the multi-spacecraft methods have the same resolution in all spatial directions which is important for detailed studies. During this day there was a long interval of ULF wave activity from around 02:45 to 03:45 UT which was intermixed with short intervals of other fluctuations. This case study is focused on the time inerval from 03:00 to 03:10 UT.

The background magnetic field, measured by FGM [2], for the chosen event was $[-4.4, 5.0, -1.7]_{\mathrm{GSE}}$ nT, so that it had a magnitude of 6.9 nT. The average solar wind velocity during this time interval was $[-525, -5, -45]_{\mathrm{GSE}}$ km/s, from the CIS-CODIF instrument [5] on Cluster spacecraft 4. Spacecraft potential measurements made by the EFW instrument can be used to estimate the plasma electron density [6], which was around $10 \mathrm{~cm}^{-3}$ for this event.

2.1. Single spacecraft analysis

The data that were used in this study are shown in Fig. 1, where the top two panels display the x and y components of the electric field and the bottom panels the three components of the magnetic field. The data for all four spacecraft are included in the plots where the data from spacecraft 1 is denoted by black, spacecraft 2 red, spacecraft 3
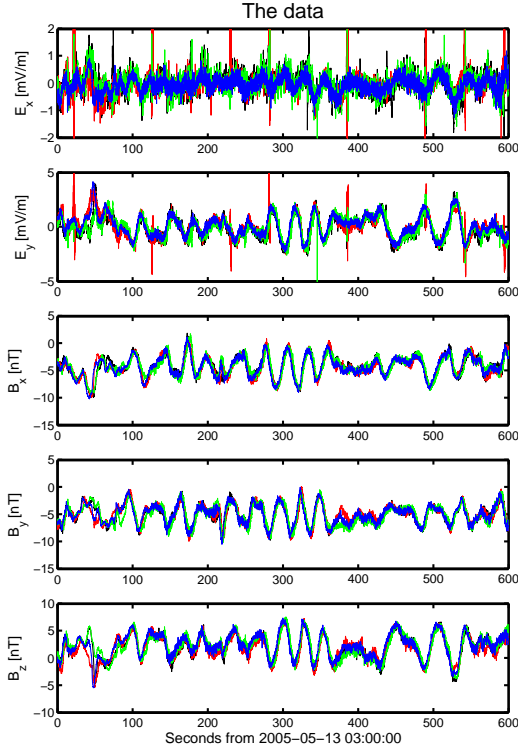
Figure 1. *The data that were used in this case study. The top two panels show the EFW electric field data in the satellite spin plane, and the bottom three panels the FGM magnetic field data. All data are displayed using the DS coordinate system. The colours are black for spacecraft 1, red for spacecraft 2, green for spacecraft 3 and blue for spacecraft 4.*

green and spacecraft 4 blue. We use the despun (DS) coordinate system for this plot because this is the natural system for the EFW instrument. The physically more relevant GSE coordinate system is also used in this text.

The electric field data have been prepared in order to remove effects from satellite induced asymmetries of the plasma [7] which means that also the background electric field has been removed in the plots. The regularly occuring spikes that are seen in these data come from the WHISPER instrument [8] when it is in active mode. They will affect the data at high frequencies, but since we will only consider very low frequencies we can ignore these spikes. There is considerably more noise in the sunward (x) component of the electric field, which comes from the previously mentioned asymmetries of the plasma surrounding the spacecraft. Also note that the x and y components are displayed using different scales.

We see that the four spacecraft had very similar time series during this interval, and that there were periods of clear low frequency oscillations. These oscillations had a period of about 30 s and the magnetic fluctuations had amplitudes of the same order of magnitude as the background magnetic field.
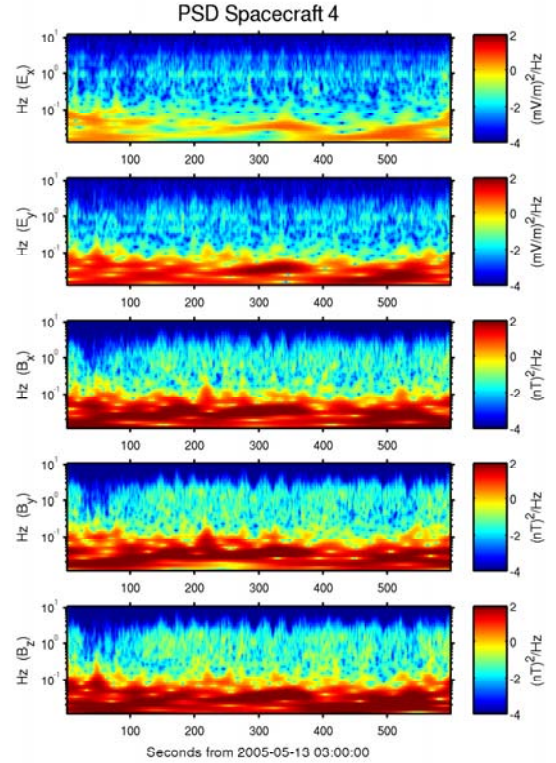

Figure 2. *Spectrograms of the data in Fig. 1 for spacecraft 4. They have been calculated using a Morlet wavelet transform.*

Spectrograms of the data from spacecraft 4 are displayed in Fig. 2. These have been calculated using a continuous Morlet wavelet transform. From these spectrograms, it is clear that there was indeed a maximum of the wave energy around 0.03 Hz also at periods when the low frequency oscillations were not clear. There was also a clear difference in the maximum value of the power spectral density between the two electric field components. The results were similar for all four spacecraft.

It is also interesting to study the power spectra for the data averaged over the whole time interval. Here we see the maximum at 0.03 Hz but there were in addition also hints of a second maximum between 1 and 2 Hz.

The polarisation [9] of the wave magnetic field of spacecraft 4 with respect to the background magnetic field is shown in Fig. 4. The panels show the spectral intensity, the ellipticity and the tilt angle of the Here the ellipticity is defined so that a value of 0 corresponds to a linear polarised wave while the values $+1$ and -1 correspond to right-handed and left-handed circular polarisation respectively. The tilt angle is defined to be twice the angle between the major axis of the polarisation ellipse and the first coordinate axis.

We see clearly in Fig. 4 that the 0.03 Hz wave was left-handed circularly polarised, except for for a short period at the beginning of the interval. Also the higher frequency waves seemed to be left-handed circular polarised. We
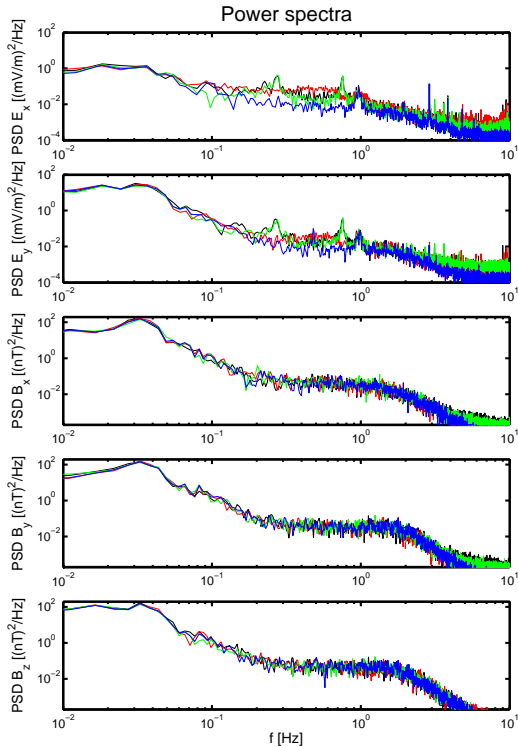
Figure 3. The power spectra of the data in Fig. 1 averaged over the whole 10 minute time interval.
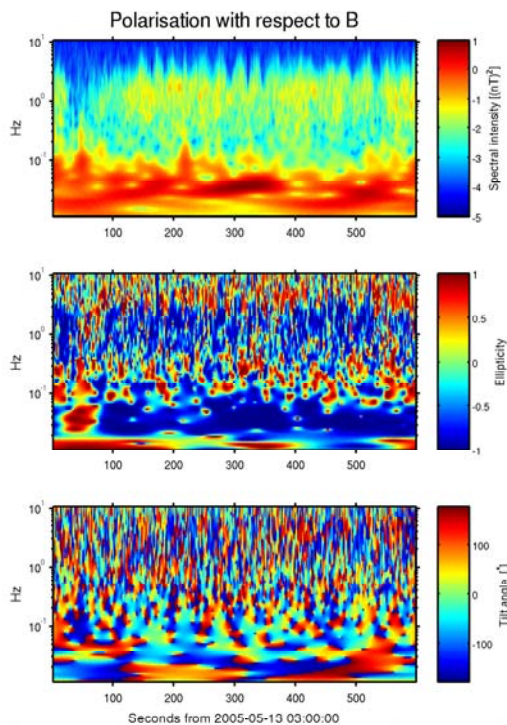

Figure 4. The polarisation of the wave magnetic field of spacecraft 4 with respect to the background magnetic field. The ellipticity is defined so that $+1$ means right-handed and -1 left-handed circular polarisation.

must note, however, that this polarisation was determined in the spacecraft frame of reference. The polarisation in the plasma frame of reference is more interesting to study if we want to compare the results with theoretical results. The tilt angle plot does not say us anything in this study since the wave polarisation was close to circular and hence the tilt angle direction was poorly defined.

When performing minimum variance analysis (MVA) [10] on the wave magnetic field data we found that the direction of the wave vector for the 0.03 Hz wave was $\pm[-0.54, 0.66, -0.50]_{\mathrm{GSE}}$. The MVA technique gives similar results when applied to the magnetic field data of the other satellites.

There is a sign ambiguity from MVA in the calculated direction of the wave-vector and we do not know its norm, and hence not the wavelength. This is a big problem since it prevents us from finding the frequencies and the polarisation in the plasma frame of reference. If we do not include any assumptions of the nature of the ULF waves we instead need to use multi-spacecraft methods to resolve this.

2.2. Multi-spacecraft analysis

There was good coherence between the satellite data at 0.03 Hz. We could thus study the phase difference for these waves between the spacecraft to estimate their wave vector [11], assuming that these were plane waves. For the z component of the magnetic field the wave vector was then estimated to be around $[-0.35, 0.39, -0.32]_{\mathrm{GSE}} \times 10^{-3}$ rad/km, corresponding to a wavelength of about 10,000 km. This is a factor 10 larger than the spacecraft separation distance which is a bit much for having good accuracy for these measurements. Similar results could be obtained for the four other measured components of the electromagnetic field. The results here were calculated under the assumption that there was only one wave present with the frequency 0.03 Hz. This assumption had to be verified and that could be done using the k-filtering method.

The higher frequency component could not be analysed in this way because there was too low coherency between the different spacecraft at those frequencies. The spacecraft separation was in other words too large in this case for this kind of analyis of these waves.

2.3. The k-filtering technique

The k-filtering technique [1] is a multi-spacecraft analysis method which enables the estimation of the wave-field energy distribution, P, as a function of frequency, ω, and wave-vector, $\vec{k}$. It may thus be used to check if there are more than one wave-mode at a given frequency. The cen-

tral equation of this method is [12]

$$P(\omega, \vec{k}) = \text{Trace} \left\{ \bar{\bar{C}} \left(\bar{\bar{C}}^\dagger \bar{\bar{H}}^\dagger \bar{\bar{M}}^{-1} \bar{\bar{H}} \bar{\bar{C}} \right)^{-1} \bar{\bar{C}}^\dagger \right\}. \quad (1)$$

We will not go into a detailed derivation of this equation but its components will be described here. $\bar{\bar{M}}(\omega)$ is the spatial correlation matrix. It includes the measured data from all four spacecraft. $\bar{\bar{H}}(\vec{k})$ is a matrix that is calculated from the relative spacecraft positions. Finally $\bar{\bar{C}}(\omega, \vec{k})$ is the constraining matrix. It includes the physics that the waves are expected to satisfy, and it is included in the equation so that non-physical results may be excluded. We were using electric and magnetic field measurements in this study so we used a constraining matrix based on the Faraday induction law here.

The k-filtering technique has to be modified slightly to allow for realistic Cluster wave magnetic and electric field data [7]. These modifications had previously been applied on the combined EFW and STAFF-SC (magnetic) [13] data on frequencies above 0.35 Hz [7]. The method was in this study extended to lower frequencies by using FGM measurements for the magnetic field data.

Fig. 5 shows iso-surface plots of the wave energy density in wave vector space for the frequency 0.03 Hz. The heart-shaped object in the center of the left hand panel displays the locations in wave vector space where the wave energy density is half of the maximum at this frequency. The box in that panel is included to indicate the spatial aliasing properties for the spacecraft constellation at hand [7]. The fact that the half-energy surface is small compared to this box indicates that the waves were well focused in wave vector space during this time period.

The right hand panel of Fig. 5 is a closer look at the central parts of the left hand panel. The outer surface is the same and the inner surface corresponds to 88% of the maximum wave energy density. We can see that there was in principle only one wave-vector present for the 0.03 Hz waves so the assumption made in the previous section was valid. The single maximum of the wave energy distribution at this frequency in the spacecraft frame of reference had the wave vector $[-0.29, 0.60, -0.22]_{\text{GSE}} \times 10^{-3}$ rad/km, which corresponds to a wavelength of about 9000 km.

In Fig. 6 we have chosen a k_z value of -0.22×10^{-3} rad/km and display the iso-contours of the wave energy density in the k_x-k_y plane for this value of k_z as white lines. This kind of plot is of interest especially when the wave field is more complex than the one in this example. This visualisation method is in such cases a good way of distinguishing different maxima of the wave energy density. The background colour indicates the ratio between the wave magnetic and electric field energy densities. That is useful in the investigation of the nature of the measured plasma fluctuations.

3. WAVE MODE IDENTIFICATION

We are now in a position where we can calculate the characteristics of the low frequency wave mode in the plasma frame of reference. The frequency of a wave in the plasma frame of reference is calculated from

$$f_{\text{plasma}} = \left| f_{\text{sc}} - \frac{1}{2\pi} \vec{v} \cdot \vec{k}_{\text{sc}} \right|, \quad (2)$$

where f_{sc} is the wave frequency and $\vec{k}_{\text{sc}}$ the wave vector in the spacecraft frame of reference. $\vec{v}$ is the plasma velocity with respect to the spacecraft. From this expression it is easy to calculate the phase velocity of the wave in the plasma frame of reference:

$$\vec{v}_{\text{ph,plasma}} = \frac{2\pi f_{\text{sc}} - \vec{v} \cdot \vec{k}_{\text{sc}}}{k_{\text{sc}}^2} \vec{k}_{\text{sc}}. \quad (3)$$

We note that if the nominator in this equation is negative, the phase velocity is in the opposite direction in the plasma frame of reference compared with the spacecraft frame. This may happen when the wave is propagating upstream in the plasma frame but is convected downstream by the plasma flow. Additional results from this are changes of the wave polarisation so that a right-handed wave in the plasma frame of reference, for instance, would be measured as a left-handed wave by the spacecraft.

Using the wave-vector determined by the k-filtering technique the frequency of the 0.03 Hz wave could be calculated to be 0.0046 Hz in the plasma frame of reference. The wave polarisation was in this case not changed by the change of reference frames and was thus left-handed circular also in the plasma frame. The phase velocity of the wave was 50 km/s with respect to the plasma which was comparable with the Alfvén velocity (about 45 km/s in this plasma). Finally the angle of propagation with respect to the background magnetic field was 16°. We could thus find that the ULF wave studied here had the characteristics of a shear Alfvén wave, also called the intermediate wave. This wave was propagating downstream in the plasma and, since it is convected with the plasma, its phase velocity and hence also its frequency in the spacecraft frame of reference was increased.

4. CONCLUSIONS

We have analysed an ULF wave event at the Earth's foreshock using the four Cluster spacecraft. Measurements from the individual satellites was used to determine the frequency and the polarisation of the waves in the spacecraft frame of reference, where the waves were found to have the frequency 0.03 Hz and to be left-handed circular polarised. By applying multi-spacecraft methods we were able to estimate the wave-vector of these waves, and this knowledge was used to calculate the characteristics of the waves in the plasma frame of reference. In the
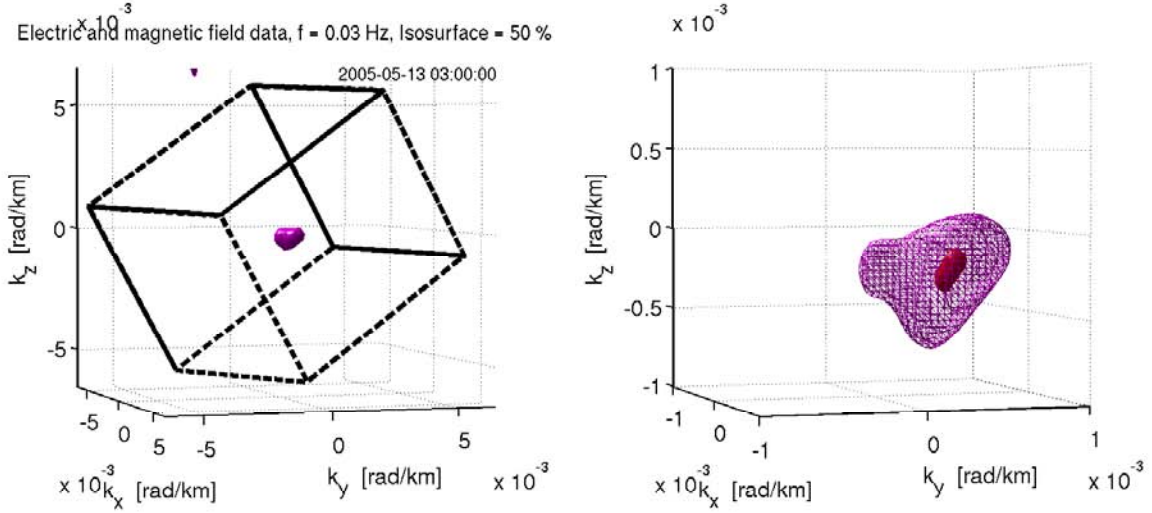
Figure 5. Iso-surfaces for the wave energy density in wave vector space at 0.03 Hz. The box in the left hand figure is included to indicate the spatial aliasing properties. The right hand figure is a closer look at the central part of the left hand figure.
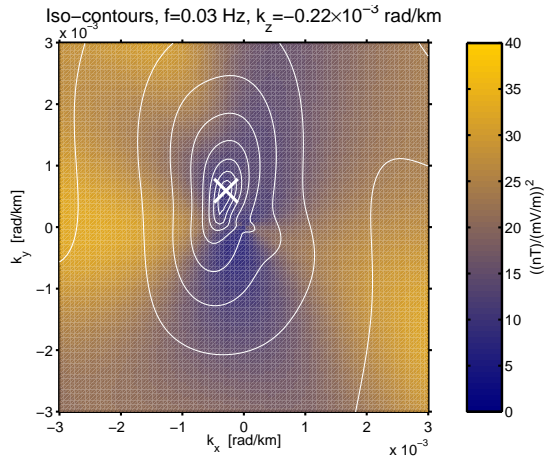

Figure 6. Iso-contours of the wave energy density at 0.03 Hz for $k_z = -0.22 \times 10^{-3}$ rad/km. The background colour is given by the ratio between the magnetic and the electric parts of the wave energy density.

plasma frame the waves had the frequency 0.046 Hz with a phase velocity close to the Alfvén velocity. They had left-handed circular polarisation and were propagating quasi-parallel to the background magnetic field, which means that these waves seemed to be shear Alfvén waves.

We also found that the k-filtering technique is a good complement to other techniques for the investigation of ULF waves in the Earth's foreshock but it was not crucial in this case study where the wave field was simple. Another thing to note from this study is that the simultaneous multi-spacecraft analysis of both the 0.03 Hz waves and the higher frequency waves is not possible here. We would need two different spacecraft separation scales for that kind of analysis.

REFERENCES

1. Pinçon, J. L. and Lefeuvre, F. Local characterization of homogeneous turbulence in a space plasma from simultaneous measurements of field components at several points in space. *J. Geophys. Res.*, 96(A2):1789–1802, February 1991.

2. Balogh, A., Carr, C. M., Acuña, M. H., Dunlop, M. W., Beek, T. J., Brown, P., Fornacon, K.-H., Georgescu, E., Glassmeier, K.-H., Harris, J., Musmann, G., Oddy, T., and Schwingenschuh, K. The Cluster magnetic field investigation: overview of in-flight performance and initial results. *Ann. Geophysicae*, 19(10/12):1207–1217, 2001.

3. André, M., Behlke, R., Wahlund, J.-E., Vaivads, A., Eriksson, A. I., Tjulin, A., Carozzi, T. D., Cully, C., Gustafsson, G., Sundkvist, D., Khotyaintsev, Y., Cornilleau-Wehrlin, N., Rezeau, L., Maksimovic, M., Lucek, E., Balogh, A., Dunlop, M., Lindqvist, P.-A., Mozer, F., Pedersen, A., and Fazakerley, A. Multi-spacecraft observations of broadband waves near the lower hybrid frequency at the Earthward edge of the magnetopause. *Ann. Geophysicae*, 19:1471–1481, 2001.

4. Robert, P., Roux, A., Harvey, C. C., Dunlop, M. W., Daly, P. W., and Glassmeier, K.-H. Tetrahedron geometric factors. In Paschmann, G. and Daly, P. W., editors, *Analysis methods for multi-spacecraft data*, ISSI Scientific Report SR-001, chapter 13, pages 323–348. ISSI/ESA, 1998.

5. Rème, H., Aoustin, C., Bosqued, J. M., Dandouras, I., Lavraud, B., Sauvaud, J. A., Barthe, A., Bouyssou, J., Camus, T., Coeur-Joly, O., Cros, A., Cuvilo, J., Ducay, F., Garbarowitz, Y., Medale, J. L., Penou, E., Perrier, H., Romefort, D., Rouzaud, J., Vallat,

6

C., Alcaydé, D., Jacquey, C., Mazelle, C., d'Uston, C., Möbius, E., Kistler, L. M., Crocker, K., Granoff, M., Mouikis, C., Popecki, M., Vosbury, M., Klecker, B., Hovestadt, D., Kucharek, H., Kuenneth, E., Paschmann, G., Scholer, M., Sckopke, N., Seidenschwang, E., Carlson, C. W., Curtis, D. W., Ingraham, C., Lin, R. P., McFadden, J. P., Parks, G. K., Phan, T., Formisano, V., Amata, E., Bavassano-Cattaneo, M. B., Baldetti, P., Bruno, R., Chionchio, G., Di Lellis, A., Marcucci, M. F., Pallocchia, G., Korth, A., Daly, P. W., Graeve, B., Rosenbauer, H., Vasyliunas, V., McCarthy, M., Wilber, M., Eliasson, L., Lundin, R., Olsen, S., Shelley, E. G., Fuselier, S., Ghielmetti, A. G., Lennartsson, W., Escoubet, C. P., Balsiger, H., Friedel, R., Cao, J.-B., Kovrazhkin, R. A., Papamastorakis, I., Pellat, R., Scudder, J., and Sonnerup, B. First multispacecraft ion measurements in and near the Earth's magnetosphere with the identical Cluster ion spectrometry (CIS) experiment. *Ann. Geophysicae*, 19:1303–1354, 2001.

6. Pedersen, A. Solar wind and magnetosphere plasma diagnostics by spacecraft electrostatic potential measurements. *Ann. Geophysicae*, 13(2):118–129, 1995.

7. Tjulin, A., Pinçon, J.-L., Sahraoui, F., André, M., and Cornilleau-Wehrlin, N. The k-filtering technique applied to wave electric and magnetic field measurements from the Cluster satellites. *J. Geophys. Res.*, Accepted for publication, 2005.

8. Décréau, P. M. E., Fergeau, P., Krasnosel'skikh, V., Lévèque, M., Martin, P., Randriamboarison, O., Sené, F. X., Trotignon, J. G., Canu, P., and Mögensen, P. B. Whisper, a resonance sounder and wave analyser: Performances and perspectives for the Cluster mission. *Space Sci. Rev.*, 79:157–193, 1997.

9. Carozzi, T. D., Thidé, B., Leyser, T. B., Komrakov, G., Frolov, V., Grach, S., and Sergeev, E. Full polarimetry measurements of stimulated electromagnetic emissions: First results. *J. Geophys. Res.*, 106(A10):21395–21407, 2001.

10. Sonnerup, B. U. Ö. and Cahill, Jr, L. J. Magnetopause structure and attitude from Explorer 12 observations. *J. Geophys. Res.*, 72:171–183, 1967.

11. Dudok de Wit, T., Krasnosel'skikh, V. V., Bale, S. D., Dunlop, M. W., Lühr, H., Schwartz, S. J., and Woolliscroft, L. J. C. Determination of dispersion relations of quasi-stationary plasma turbulence using dual satellite data. *Geophys. Res. Lett.*, 22(19):2653–2656, 1995.

12. Pinçon, J.-L. and Motschmann, U. Multi-spacecraft filtering: General framework. In Paschmann, G. and Daly, P. W., editors, *Analysis methods for multi-spacecraft data*, ISSI Scientific Report SR-001, chapter 3, pages 65–78. ISSI/ESA, 1998.

13. Cornilleau-Wehrlin, N., Chauveau, P., Louis, S., Meyer, A., Nappa, J. M., Perraut, S., Rezeau, L., Robert, P., Roux, A., de Villedary, C., de Conchy, Y., Friel, L., Harvey, C. C., Hubert, D., Lacombe, C., Manning, R., Wouters, F., Lefeuvre, F., Parrot, M., Pinçon, J. L., Poirier, B., Kofman, W., and Louarn, P. The Cluster spatio-temporal analysis of field fluctuations (STAFF) experiment. *Space Sci. Rev.*, 79:107–136, 1997.